

# Performance Analysis of Diagonal Eigenvalue Unity (DEU) Code Using NAND Subtraction and Spectral Direct Detection Techniques and Its Use with Triple-Play-Services in SAC-OCDMA

Salwa Mostafa<sup>1</sup> · Abd El-Naser A. Mohamed<sup>1</sup> ·

Fathi E. Abd El-Samie<sup>1</sup> ·

Ahmed Nabih Zaki Rashed<sup>1</sup>

Published online: 1 July 2015

© Springer Science+Business Media New York 2015

**Abstract** In this paper, we investigate the performance of optical code division multiple access system using the diagonal eigenvalue unity (DEU) code as a promising code for future optical networks. A comparison between the utilization of the NAND subtraction detection technique and the spectral direct detection (SDD) technique is presented to investigate which one provides better performance with the DEU code. In addition, a complete mathematical analysis for the two cases is presented. The performance of the two techniques is evaluated in terms of signal to noise ratio, bit error rate (BER), the effective received power, and phase induced intensity noise. Also, the variable weight DEU code is discussed. It demonstrates success for triple-play services (audio, video, and data) using the SDD technique to provide different quality of service (QoS) values to users. The results show that the SDD technique supports a larger number of users, reduces the receiver complexity, and provides better performance than the NAND subtraction technique. For a minimum acceptable BER of  $10^{-9}$  for a telecommunication system, the direct detection technique supports 265 users, while the NAND subtraction supports 150 users only for (weight  $W = 3$ ). Also, with variable weights in a single system, the performance of users with high weight is always better compared to that of lower weight users.

**Keywords** Spectral amplitude coding optical code division multiple access (SAC-OCDMA) · Multiple access interference (MAI) · Phase induced intensity noise (PIIN) · Diagonal eigenvalue unity (DEU) · Variable weight (VW)

---

✉ Salwa Mostafa  
salwamostafa@gmail.com

Fathi E. Abd El-Samie  
fathi\_sayed@yahoo.com

Ahmed Nabih Zaki Rashed  
ahmed\_733@yahoo.com

<sup>1</sup> Department of Electronics and Electrical Communications, Faculty of Electronic Engineering, Menoufia University, Menouf 32952, Egypt

## 1 Introduction

Optical CDMA systems are divided into two categories depending on the manner in which a specific user's code encodes an optical signal. These classifications are coherent and incoherent OCDMA. In a coherent OCDMA system, a specific user's code is applied to encode the phase of an optical signal generated from an extremely coherent broadband source. Thus, the receiver depends on coherent reconstruction of the optical signal to obtain the user's information and the phase of carriers must be known. Also, a coherent system uses unipolar codewords. On the other hand, an incoherent OCDMA system depends on manipulating the amplitude of the optical signal and uses bipolar codewords. So, the receiver relies on an incoherent decoding and the knowledge of phase information is unnecessary. Also, the hardware complexity is reduced. Therefore, we use an incoherent system in this study [1].

In OCDMA systems, the main factors that degrade system performance and reduce the number of active users are the multiple access interference (MAI) and the PIIN produced from overlapping of spectra from various active users in the system. In the OCDMA system, the detection process plays a critical role in the design of transmitters and receivers to eliminate MAI and reduce PIIN. Thus, several detection techniques are used such as complementary, AND, NAND [2], XOR [3] subtraction techniques, and the spectral direct detection (SDD) techniques [4]. They are used with SAC-OCDMA, where every user is allocated a distinct codeword to encode the spectral amplitude of an optical source and represent its address. The SAC is one of the techniques used to reduce the MAI effect by using fixed cross correlation codes. It offers better transmission performance than time spreading coding and spectral phase coding (SPC).

The SDD technique is the best detection technique, because it detects clean chips only, eliminating MAI and reducing the receiver cost and complexity as the number of filters needed is decreased. However, this technique provides inefficient treatment to the MAI problem [5] because it does not use the full weight of the user at the receiver. On the other hand, the NAND provides better performance than complementary, AND, and XOR, because it produces higher weight. High weight means high power received signals, which in turn produces better SNR [2]. Complementary and AND subtraction remove MAI, but provide poor signal quality. Also, these subtraction techniques increase the receiver complexity and cost, because the number of filters and detectors is twice that needed by the SDD but they provide an efficient treatment to the MAI problem [5] by detecting the full weight of the code sequence.

OCDMA is a suitable solution to support different QoS values to different services by adopting variable weights in a single system to users based on demand and requirement for applications such as metro networks [6]. Users with high weight have high priority in transmission and good performance as the higher weight means a higher received power. Some studies discussed variable weight OCDMA such as integer lattice optical orthogonal code (IL-OOC) [7], variable weight OOC [8], variable weight zero cross correlation code (ZCC) [9]. In addition, triple-play services use the random diagonal (RD) code, where PIIN is suppressed using a variable weight system. Codes with larger weight have lower BER despite the long code length [10]. In the study on service differentiation using Khazani-Syed (KS) code, the authors clarified that the optimal system performance with a particular weight is obtained with an appropriate choice of the number of active users, and the overall performance is improved when the number of users with the largest weight is small in a variable weight system [11].

The contribution of this paper is to investigate the utilization of the NAND subtraction detection technique and the SDD technique for the DEU code. A detailed mathematical analysis for the two techniques with the DEU code is presented. The variable weight for the DEU code is discussed to support different QoS values to users. The properties and construction of the DEU code and its variable weight are discussed in Sect. 2. The NAND subtraction technique and the SDD technique are introduced in Sect. 3. The mathematical analysis of the DEU code for both techniques and for its variable weight using the SDD technique is given in Sect. 4. The obtained results are discussed in Sect. 5. In Sect. 6, the network simulation using optiwave.13 is given. Finally, concluding remarks are given in Sect. 7.

## 2 Code Construction

The DEU code construction depends on Jordan Block matrix [3]. This code has a simple construction, an ideal cross correlation of  $0 \leq \lambda c \leq 1$ , the ability to support a high number of users, and free cardinality in selecting the code weight and the number of users. These characteristics make DEU code a promising code for use in future OCDMA networks [3].

Steps of code construction [3]

*Step 1* Compute the positions of ones in the successive super diagonal (SSD).

$$\text{The positions of ones in the SSD} = \{(\dot{r}, \dot{r}W - (\dot{r} + W - 3)), (\dot{r}, \dot{r}W - (\dot{r} + W - 4)), (\dot{r}, \dot{r}W - (\dot{r} + W - 5)), \dots\} \quad (1)$$

where  $\dot{r}$  is the row number  $\dot{r} = 1, 2, 3, \dots, N$ , and  $W$  is the code weight.

*Step 2* Compute the positions of ones in the Main Diagonal (MD) using

$$\text{MD} = (\dot{r}, (W - 1)\dot{r} - 2). \quad (2)$$

*Step 3* Compute the length of code for the basic matrix  $L_B$  using

$$L_B = N_B(W - 1) + 1. \quad (3)$$

*Step 4* Compute the DEU basic matrix with dimensions  $N_B \times L_B$ .

*Step 5* Put 1 s at the positions of  $(\text{MD})_K$  and  $(\text{SSD})_K$  in the DEU basic matrix and complete the empty spaces with 0's at  $L - W$

To support a higher number of users, use the mapping technique  $m = N/N_B$

*Example* Case (even, even) ( $W = 4, N_B = 8$ )

*Step 1* Compute the positions of ones in the Successive Super Diagonal (SSD)

Based on Eq. (1), the positions of ones in the SSD are as follows:

For  $\dot{r} = 1$  "1"s positions  $\{(1, 2)(1, 3)(1, 4)\}$      $\dot{r} = 2$  "1"s positions  $\{(2, 5)(2, 6)(2, 7)\}$   
 $\dot{r} = 3$  "1"s positions  $\{(3, 8)(3, 9)(3, 10)\}$      $\dot{r} = 4$  "1"s positions  $\{(4, 11)(4, 12)(4, 13)\}$   
 $\dot{r} = 5$  "1"s positions  $\{(5, 14)(5, 15)(5, 16)\}$      $\dot{r} = 6$  "1"s positions  $\{(6, 17)(6, 18)(6, 19)\}$   
 $\dot{r} = 7$  "1"s positions  $\{(7, 20)(7, 21)(7, 22)\}$      $\dot{r} = 8$  "1"s positions  $\{(8, 23)(8, 24)(8, 25)\}$

Step 2: Compute the positions of ones in the main diagonal (MD).

- For  $\dot{r} = 1$  "1"'s positions in MD = (3, 7)     $\dot{r} = 2$  "1"'s positions in MD = (4, 10)
- $\dot{r} = 3$  "1"'s positions in MD = (3, 7)     $\dot{r} = 4$  "1"'s positions in MD = (4, 10)
- $\dot{r} = 5$  "1"'s positions in MD = (5, 13)     $\dot{r} = 6$  "1"'s positions in MD = (6, 16)
- $\dot{r} = 7$  "1"'s positions in MD = (7, 19)     $\dot{r} = 8$  "1"'s positions in MD = (8, 22)

Step 3 Compute the length of code for the basic matrix  $L_B$  using  $L_B = N_B (W - 1) + 1 = 8(4 - 1) + 1 = 25$ .

Step 4 Compute the DEU basic matrix with dimensions  $N_B \times L_B = 8 \times 25$ .

Step 5 Put 1 s in the positions of  $(MD)_K$  and  $(SSD)_K$  in the DEU basic matrix and complete the empty spaces with 0's. DEU Code for ( $W = 4, N_B = 8, L_B = 25$ )

$$\begin{bmatrix} 1 & 1 & 1 & 1 & 0 & 0 & 0 & 0 & 0 & 0 & 0 & 0 & 0 & 0 & 0 & 0 & 0 & 0 & 0 & 0 & 0 & 0 & 0 \\ 0 & 0 & 0 & 1 & 1 & 1 & 1 & 0 & 0 & 0 & 0 & 0 & 0 & 0 & 0 & 0 & 0 & 0 & 0 & 0 & 0 & 0 & 0 \\ 0 & 0 & 0 & 0 & 0 & 0 & 1 & 1 & 1 & 1 & 0 & 0 & 0 & 0 & 0 & 0 & 0 & 0 & 0 & 0 & 0 & 0 & 0 \\ 0 & 0 & 0 & 0 & 0 & 0 & 0 & 0 & 0 & 1 & 1 & 1 & 1 & 0 & 0 & 0 & 0 & 0 & 0 & 0 & 0 & 0 & 0 \\ 0 & 0 & 0 & 0 & 0 & 0 & 0 & 0 & 0 & 0 & 0 & 0 & 0 & 1 & 1 & 1 & 1 & 0 & 0 & 0 & 0 & 0 & 0 \\ 0 & 0 & 0 & 0 & 0 & 0 & 0 & 0 & 0 & 0 & 0 & 0 & 0 & 0 & 0 & 0 & 1 & 1 & 1 & 1 & 0 & 0 & 0 \\ 0 & 0 & 0 & 0 & 0 & 0 & 0 & 0 & 0 & 0 & 0 & 0 & 0 & 0 & 0 & 0 & 0 & 0 & 0 & 1 & 1 & 1 & 1 \end{bmatrix}$$

### 2.1 Construction of Variable Weight DEU Code

There are three main kinds of information (audio, video, and data). We will use three weights (2, 4, 6) to differentiate the QoS required for each of them. Higher weight means better quality transmission for the information requiring high priority. The weight choice depends on the signal quality needed. Different detection techniques used in the single weight system can be applied to a variable weight system. The following example illustrates the implementation of variable weight in a system using the SDD technique. We suppose three different services, each with a specific code weight and a different number of subscribers. We used two users of weight 2 requesting audio, four users of weight 4 needing video, and six users of weight 6 demanding data. The codes of various weights must be organized in a manner that maintains a cross correlation always equal to one. Zeroes are inserted after and before the original codes to fill and merge various weights into the system. The construction of the DEU code with variable weight is shown below. The mapping technique can be used to increase the number of users for each weight if needed [6, 9]. The total code length is equal to the sum of code lengths required for each weight  $L_T = L(2) + L(4) + L(6)$

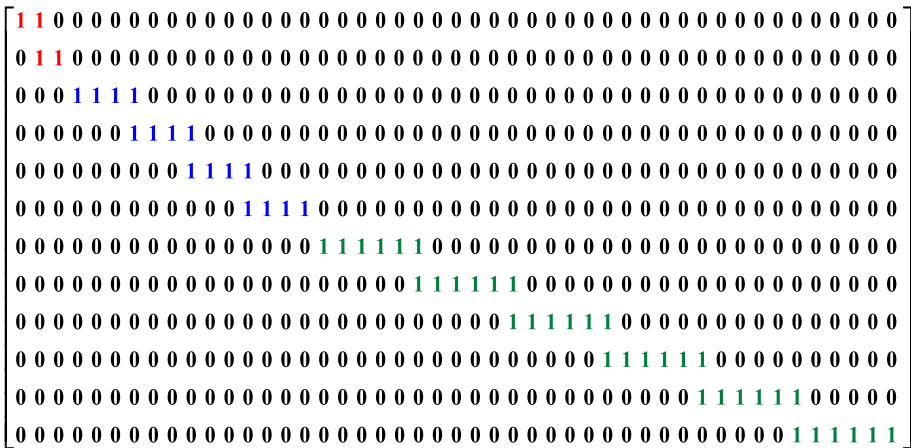
For  $W = 2$ , the number of users  $N_B = 2$ , the code length  $L_B = 3$ .

For  $W = 4$ , the number of users  $N_B = 4$ , the code length  $L_B = 13$ .

For  $W = 6$ , the number of users  $N_B = 6$ , the code length  $L_B = 31$ .

The total code length  $L_T = 47$

$$\begin{bmatrix} \begin{bmatrix} W = 2 & N_B = 2 \\ L_B = 3 \end{bmatrix} & 0 & 0 \\ 0 & \begin{bmatrix} W = 4 & N_B = 4 \\ L_B = 13 \end{bmatrix} & 0 \\ 0 & 0 & \begin{bmatrix} W = 6 & N_B = 6 \\ L_B = 31 \end{bmatrix} \end{bmatrix}$$



### 3 Detection Techniques

#### 3.1 NAND Subtraction Detection Technique

Figure 1 shows that the transmitter consists of an encoder that is used for encoding the pulses of an optical source corresponding to every user code sequence to generate a codeword distinct for each user address. Then, the data are modulated by an external modulator and multiplexed together to send through an optical fiber. At the receiver side, the received signal is separated into two sections, one decoded by an optical filter the same as that used in the encoder and the other by a decoder that has a NAND filter structure. Then, the detection is performed by two PIN photo-detectors PD<sub>1</sub> and PD<sub>2</sub>. The electrical signal in the low arm is subtracted from that of the top arm to eliminate MAI [2]. The subtraction techniques increase the receiver complexity and cost, but provide reliability in treating the MAI problem by using the full weight in the user code sequence and eliminating the MAI. Logic gates are used as operations not as digital gates. For example, in Table 1, for the two code sequences *x* and *y*, the complementary, AND, XOR, and NAND operations are instituted. The NAND subtraction  $\tilde{x}\tilde{y}$  represents the operation of NAND between the *x* and *y* code sequences.  $\lambda_i$  represents the spectral positions of the chips. As shown, the NAND subtraction detection technique produces larger weights than complementary, AND, and XOR subtraction. When the weight of the code is increased, the signal power is also increased, hence, the SNR is increased. So, the performance of the OCDMA

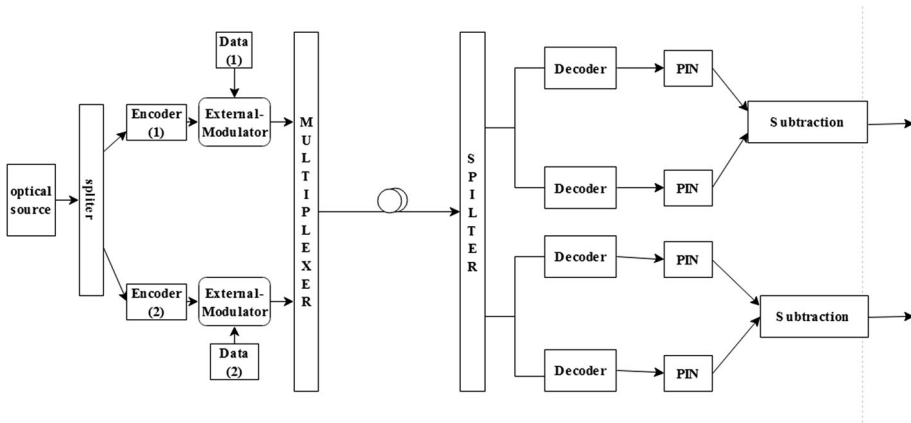


**Fig. 1** OCDMA system architecture using the NAND subtraction detection technique [2]

system is improved. At the receiver side, the interference from other users is cancelled and the subtractor output cross correlation  $Z$  is expressed as [5]

$$Z_{NAND} = \theta_{xy} - \theta_{(\sim xy)y} = 0 \tag{4}$$

$$Z_{AND} = \theta_{xy} - \theta_{(x\&y)y} = 0 \tag{5}$$

$$Z_{XOR} = \theta_{xy} - \theta_{(x\oplus y)y} = 0 \tag{6}$$

$$Z_{Complementary} = \theta_{xy} - \theta_{x\bar{y}} = 0 \tag{7}$$

where  $\theta_{xy}$  is the cross-correlation written as [12]

$$\theta_{xy} = \sum_{i=0}^L x_i y_i \tag{8}$$

### 3.2 Spectral Direct Detection Technique

As shown in Fig. 2, with the SDD technique, the transmitter is similar to that used in the NAND subtraction technique. The receiver consists of a splitter used to separate incoming signals, a decoder, an optical filter to decode the non-overlapping chips only for the desired user, and a PIN photodiode. In this technique, the clean chips (non-overlapping chips) only are detected, because the data are supposed to be sufficiently recovered from all the chips that do not interfere with other chips from different code sequences. So, there is no need to use any subtraction technique to remove interference from other active users (overlapping chips) [4]. Thus, the number of filters is reduced. Both the cost and complexity of the system are reduced, also. Using the SDD technique, we can eliminate the MAI and PIIN effects. As a result, the overall system performance in terms of SNR and BER is improved. However, it provides a weak treatment to the MAI issue by detecting clean chips only in the code sequence [5]. Hence, the complete potential of code weight is not realized, where the more chips received and detected mean more received power. For example, we can let the code have a weight of 4 and a number of clean chips of only 2. At the receiver side, we

**Table 1** Comparison between complementary, AND, NAND and XOR operations between two code sequences x and y

	$X$	1	1	1	1	0	0	0	0	0	0	0	0	0	0	0	0	0	0
	$Y$	0	0	0	1	1	1	1	0	0	0	0	0	0	0	0	0	0	0
	$xy$	0	0	0	1	0	0	0	0	0	0	0	0	0	0	0	0	0	0
NAND	$\tilde{x}y$	1	1	1	0	1	1	1	1	1	1	1	1	1	1	1	1	1	1
	$\widetilde{(xy)}y$	0	0	0	0	1	1	1	1	0	0	0	0	0	0	0	0	0	0
AND	$X\&y$	0	0	0	1	0	0	0	0	0	0	0	0	0	0	0	0	0	0
	$(X\&y)y$	0	0	0	1	0	0	0	0	0	0	0	0	0	0	0	0	0	0
XOR	$X\oplus Y$	1	1	1	0	1	1	1	1	0	0	0	0	0	0	0	0	0	0
	$(X\oplus Y)Y$	0	0	0	0	1	1	1	1	0	0	0	0	0	0	0	0	0	0
COMP.	$\bar{y}$	1	1	1	0	0	0	0	1	1	1	1	1	1	1	1	1	1	1
	$x\bar{y}$	1	1	1	0	0	0	0	0	0	0	0	0	0	0	0	0	0	0

	$X$	0	0	0	0	0	0	0	0	0	0	0	0	0	0	0	0	0	0
	$Y$	0	0	0	0	0	0	0	0	0	0	0	0	0	0	0	0	0	0
	$xy$	0	0	0	0	0	0	0	0	0	0	0	0	0	0	0	0	0	0
NAND	$\tilde{x}y$	1	1	1	1	1	1	1	1	1	1	1	1	1	1	1	1	1	1
	$\widetilde{(xy)}y$	0	0	0	0	0	0	0	0	0	0	0	0	0	0	0	0	0	0
AND	$X\&y$	0	0	0	0	0	0	0	0	0	0	0	0	0	0	0	0	0	0
	$(X\&y)y$	0	0	0	0	0	0	0	0	0	0	0	0	0	0	0	0	0	0
XOR	$X\oplus Y$	0	0	0	0	0	0	0	0	0	0	0	0	0	0	0	0	0	0
	$(X\oplus Y)Y$	0	0	0	0	0	0	0	0	0	0	0	0	0	0	0	0	0	0
COMP.	$\bar{y}$	1	1	1	1	1	1	1	1	1	1	1	1	1	1	1	1	1	1
	$x\bar{y}$	0	0	0	0	0	0	0	0	0	0	0	0	0	0	0	0	0	0

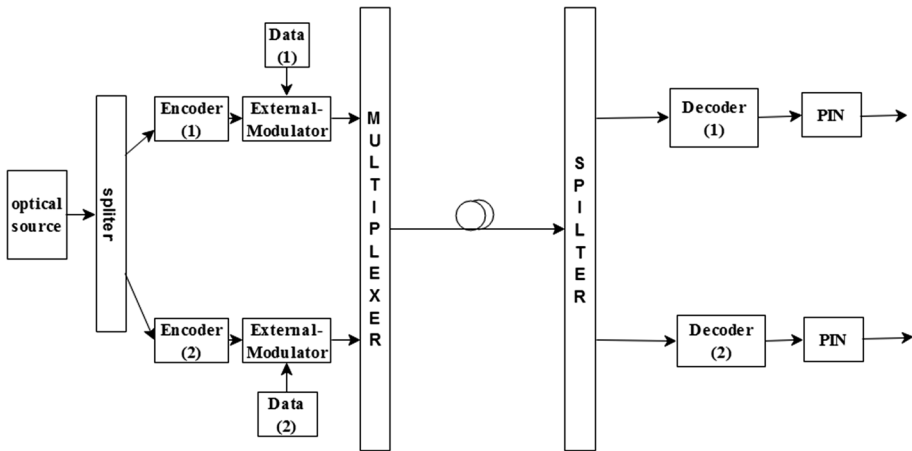


Fig. 2 OCDMA system using the direct detection technique [4]

detect only 2 chips, although we can recover data, but the small number of chips detected, means a smallpower received by the user which affects the BER. Notice that the entire code spectra still need to be sent to distinguish the signature address.

### 4 Mathematical Analysis

#### 4.1 Mathematical Analysis Using the NAND Subtraction Technique

Let  $C_N(i)$  represent the  $i$ th element of the  $N$ th DEU code sequence. The characteristics of the code for the NAND subtraction technique can be expressed as [2, 3]

$$\sum_{i=1}^L C_N(i)C_K(i) = \begin{cases} W & N = K \\ 1 & N \neq K \\ 0 & N \neq K \end{cases} \tag{9}$$

$$\sum_{i=1}^L C_N(i)\widetilde{C}_K(i)C_N(i) = \begin{cases} w & N = K \\ w - 1 & N \neq K \\ 0 & N \neq K \end{cases} \tag{10}$$

The thermal source coherent time ( $\tau_c$ ) is written as [3]

$$\tau_c = \frac{\int_0^\infty G^2(v)dv}{[\int_0^\infty G(v)dv]^2} \tag{11}$$

where  $G(v)$  is the single source sideband PSD. The variation of photocurrent due to detection of an ideally unpolarized thermal light produced by spontaneous emission can be expressed as [3, 13]

$$\sigma^2 = I_{PIN}^2 + I_{shot}^2 + I_{thermal}^2 = I^2B\tau_c + 2eIB + \frac{4K_B T_n B}{R_L} \tag{12}$$



where  $I_{PIN}^2$  indicates the phase induced intensity noise,  $I_{shot}^2$  refers to the shot noise and  $I_{thermal}^2$  is the thermal noise,  $e$  is the electron charge,  $I$  is the average photocurrent,  $I^2$  is the PSD of  $I$ ,  $B$  is the bandwidth of noise at the receiver,  $K_B$  is the Boltzmann’s constant,  $T_n$  is the noise temperature of the receiver, and  $R_L$  is the receiver load resistance.

To analyze the system, the following assumptions are used as in [13].

- (a) Each source of light is ideally unpolarized and the spectrum over the bandwidth  $[v_o - \frac{\Delta v}{2}, v_o + \frac{\Delta v}{2}]$  is flat, where  $v_o$  is the central optical frequency, and  $\Delta v$  is the light source bandwidth in hertz.
- (b) The spectral width of each power spectral component is the same.
- (c) At the receiver, each user has the same power.
- (d) Every bit stream from every user is synchronized.

The PSD of the received signal is [13]

$$r(v) = \frac{P_{sr}}{\Delta v} \sum_{n=1}^N d_n \sum_{i=1}^L C_N(i) rec(i) \tag{13}$$

$$rec(i) = \left\{ u \left[ v - v_o - \frac{\Delta v}{2L} (-L + 2i - 2) \right] - u \left[ v - v_o - \frac{\Delta v}{2L} (-L + 2i) \right] \right\} = u \left[ \frac{\Delta v}{L} \right]$$

$P_{sr}$  is the effective power at the receiver,  $N$  is the total number of users,  $L$  is the total code length.  $u(v)$  is the unit step function written as [3]

$$u(v) = \begin{cases} 1, & v \geq 0 \\ 0, & v < 0 \end{cases} \tag{14}$$

The current at PD<sub>1</sub> can be written as:

$$I_1 = R \int_0^\infty G_1(v) dv = R \int_0^\infty \frac{P_{sr}}{\Delta v} \sum_{n=1}^N d_n \sum_{i=1}^L C_N(i) C_K(i) u \left[ \frac{\Delta v}{L} \right] dv$$

$$I_1 = R \frac{P_{sr} \Delta v}{\Delta v L} W d_N + R \frac{P_{sr} \Delta v}{\Delta v L} \sum_{n=1, n \neq k}^{N_B} d_n = R \frac{P_{sr} W}{L} + R \frac{P_{sr}}{L} (N_B - 1) = R \frac{P_{sr}}{L} (W + N_B - 1) \tag{15}$$

where  $d_n$  is the data bit of the  $N$ th user that is either ‘0’ or ‘1’.

The current at PD<sub>2</sub> can be expressed with an approach similar to that in [2] as

$$I_2 = R \int_0^\infty G_2(v) dv = R \int_0^\infty \frac{P_{sr}}{\Delta v} \sum_{n=1}^N d_n \sum_{i=1}^L C_N(i) \widetilde{C}_K(i) C_N(i) u \left[ \frac{\Delta v}{L} \right] dv$$

$$I_2 = R \frac{P_{sr} \Delta v}{\Delta v L} W d_N + R \frac{P_{sr} \Delta v}{\Delta v L} (W - 1) \sum_{n=1, n \neq k}^{N_B} d_n \tag{16}$$

$$I_2 = R \frac{P_{sr}}{L} W + R \frac{P_{sr}}{L} (W - 1) (N_B - 1)$$

where  $R$  is the responsivity of the photodetector and is written as [13]

$$R = \frac{\eta e}{h \nu_c} \tag{17}$$

$\eta$  is the quantum efficiency,  $h$  is the Planks' constant,  $V_c$  is the broad-band optical pulse central frequency.

The desired user signal is the difference between the photodiodes currents, and it can be expressed as that in [13],

$$\begin{aligned}
 I &= I_2 - I_1 = R \int_0^\infty G_2(v)dv - R \int_0^\infty G_1(v)dv = \frac{P_{sr}}{L}W + \frac{P_{sr}}{L}(W - 1) \sum_{n=1n \neq k}^{N_B} d_n \\
 &\quad - \frac{P_{sr}}{L}W - \frac{P_{sr}}{L} \sum_{n=1n \neq k}^{N_B} d_n \\
 I &= \frac{P_{sr}}{L} \sum_{n=1n \neq k}^{N_B} d_n(W - 2) = \frac{P_{sr}}{L}R(W - 2)(N_B - 1)
 \end{aligned}
 \tag{18}$$

The shot noise power is expressed as [13]:

$$\begin{aligned}
 I_{shot}^2 &= 2eB(I_1 + I_2) = \left[ 2eBR \left( \int_0^\infty G_1(v)dv + \int_0^\infty G_2(v)dv \right) \right] \\
 I_{shot}^2 &= 2eBR \left( \frac{P_{sr}}{L}W + \frac{P_{sr}}{L} \sum_{n=1}^{N_B} d_n + \frac{P_{sr}}{L}W + \frac{P_{sr}}{L}(W - 1) \sum_{n=1n \neq k}^{N_B} d_n \right) \\
 I_{shot}^2 &= 2eBR \left[ \frac{P_{sr}}{L}(W + N_B - 1) + \frac{P_{sr}}{L}(W + WN_B - N_B - W + 1) \right] = \frac{2eBRP_{sr}}{L}(W + WN_B)
 \end{aligned}
 \tag{19}$$

$$\begin{aligned}
 \langle I_{PIN}^2 \rangle &= BR^2 \left[ \int_0^\infty G_1^2(v)dv + \int_0^\infty G_2^2(v)dv \right] \\
 &= \frac{BR^2 P_{sr}^2}{L\Delta v} \sum_{i=1}^L \left\{ C_K(i) \left[ \sum_{n=1}^{N_B} d_n C_n(i) \right] \cdot \left[ \sum_{m=1}^{N_B} d_m C_m(i) \right] \right\} \\
 &\quad + \frac{BR^2 P_{sr}^2}{L\Delta v} \sum_{i=1}^L \left\{ C_N(i) \widetilde{C}_K(i) \left[ \sum_{n=1}^{N_B} d_n C_n(i) \right] \cdot \left[ \sum_{m=1}^{N_B} d_m C_m(i) \right] \right\}
 \end{aligned}$$

As in [3], assume that all the users are transmitting bit "1" and  $\sum_{n=1}^N C_n \approx \frac{Nw}{L}$

$$\begin{aligned}
 \langle I_{PIN}^2 \rangle &= \frac{BR^2 P_{sr}^2}{L\Delta v} \sum_{i=1}^L \left\{ C_K(i) \frac{Nw}{L} \left[ \sum_{n=1}^{N_B} C_n(i) \right] \right\} + \frac{BR^2 P_{sr}^2}{L\Delta v} \sum_{i=1}^L \left\{ C_N(i) \widetilde{C}_K(i) \frac{Nw}{L} \left[ \sum_{n=1}^{N_B} C_n(i) \right] \right\} \\
 \langle I_{PIN}^2 \rangle &= \frac{BR^2 P_{sr}^2 Nw}{L\Delta v} \sum_{n=1}^{N_B} \left\{ \left[ \sum_{i=1}^L C_N(i) C_K(i) \right] \right\} + \frac{BR^2 P_{sr}^2 Nw}{L\Delta v} \sum_{n=1}^{N_B} \left\{ \left[ \sum_{i=1}^L C_N(i) \widetilde{C}_K(i) C_N(i) \right] \right\} \\
 I_{PIN}^2 &= \frac{BR^2 P_{sr}^2 Nw}{L^2 \Delta v} (w + N_B - 1 + w + (w - 1)(N_B - 1)) \\
 I_{PIN}^2 &= \frac{BR^2 P_{sr}^2 Nw}{L^2 \Delta v} (2w + N_B - 1 + (w - 1)(N_B - 1))
 \end{aligned}
 \tag{20}$$

The thermal noise is written as [12, 13]

$$I_{thermal}^2 = \frac{4K_b T_n B}{R_L} \tag{21}$$

The chance of transmitting bit “1” for every user is 1/2. So the SNR for DEU code using NAND detection can be expressed as

$$SNR = \frac{(I)^2}{\sigma^2} = \frac{\left[\frac{P_{sr}}{L} R(W - 2)(N_B - 1)\right]^2}{\frac{eBRP_{sr}}{L}(W + WN_B) + \frac{BR^2 P_{sr}^2 NW}{L^2 \Delta v}(2W + N_B - 1 + (W - 1)(N_B - 1)) + \frac{4K_b T_n B}{R_L}} \tag{22}$$

Using a Gaussian approach similar to that in [13], we can deduce that

$$BER = 0.5erfc\left(\sqrt{SNR/8}\right) \tag{23}$$

### 4.2 Mathematical Analysis Using the Spectral Direct Detection Technique

The code properties [4]

$$\sum_{i=1}^L C_N(i)C_K(i) = \begin{cases} W & N = K \\ 1 & N \neq K \\ 0 & N \neq K \end{cases} \tag{24}$$

The photocurrent is written as [4]

$$I_{dd} = R \int_0^\infty G_d(v)dv = R \int_0^\infty \frac{P_{sr}}{\Delta V} \sum_{n=1}^N d_n \sum_{i=1}^L C_N(i)C_K(i)u\left[\frac{\Delta v}{L}\right] dv$$

$$I_{dd} = R \frac{P_{sr}}{\Delta v} W \frac{\Delta v}{L} d_N + R \frac{P_{sr}}{\Delta v} \sum_{n=1, n \neq l}^{N_B} d_n \frac{\Delta v}{L} = R \frac{P_{sr} W}{L} + R \frac{P_{sr}}{L} (N_B - 1) = R \frac{P_{sr}}{L} (W + N_B - 1) \tag{25}$$

The sources of noise power exist in the photocurrent written as [4]

$$\sigma_d^2 = I_{shot} + I_{thermal} = 2eBI_{dd} + \frac{4K_b T_n B}{R_L}$$

$$\sigma_d^2 = 2eBR \frac{P_{sr}}{L} (W + N_B - 1) + \frac{4K_b T_n B}{R_L} \tag{26}$$

$$SNR = \frac{(I_{dd})^2}{\sigma_d^2} = \frac{\left(R \frac{P_{sr}}{L} (W + N_B - 1)\right)^2}{eBR \frac{P_{sr}}{L} (W + N_B - 1) + \frac{4K_b T_n B}{R_L}} \tag{27}$$

BER formula is as mentioned in Eq. (23).

### 4.3 Mathematical Analysis of the Variable Weight DEU Code (VW-DEU) with the SDD Technique

The SNR of a specific user with a particular weight of interest,  $W_i$  in the presence of other users with various weights using the SDD technique can be deduced in an approach similar to that in [9] to be:

$$SNR = \frac{(I_{dd})^2}{\sigma_d^2} = \frac{\left(R \frac{P_{sr}}{L_T} (W_i + N_{Bi} - 1)\right)^2}{eBR \frac{P_{sr}}{L_T} (W_i + N_{Bi} - 1) + \frac{4K_b T_n B}{R_L}} \tag{28}$$

BER formula is as that mentioned in Eq. (23)

## 5 Results and Discussion

The system performance is simulated using MATLAB. Table 2 states the parameters used in simulation.

**Table 2** System parameters [2, 3]

Parameters	Symbol	Value
Quantum efficiency	$\eta$	0.6
Planks' constant	$h$	$6.626 \times 10^{-34}$ J S
Electron charge	$e$	$1.602 \times 10^{-19}$ C
Operating wavelength	$\lambda$	1550 nm
Equivalent noise band-width	$B$	311 MHz
Effective power	$P_{sr}$	-10 dB
Broadband source linewidth	$\Delta\nu$	3.75 THz
Receiver noise temperature	$T$	300 K
Boltzmann's constant	$K_B$	$1.3807 \times 10^{-23}$ J K <sup>-1</sup>

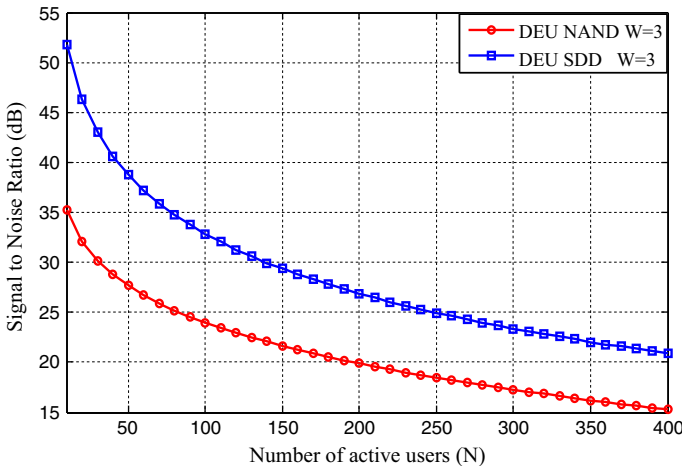


**Fig. 3** SNR versus the number of active users when  $P_{sr} = 10$  dBm  $N_B = 7$

### 5.1 Relationship Between SNR and the Number of Active Users

Figure 3 shows the relationship between the number of active users and the SNR for both the SDD technique and the NAND subtraction technique. It proves that the SDD technique provides a better performance than the NAND subtraction detection technique, because the clean chips only are detected, which eliminates both the MAI and the PIIN from the system. In contrast, using the NAND subtraction technique, the MAI is removed but the PIIN is still present in the system, which degrades its performance.

### 5.2 Relationship Between BER and the Number of Active Users

Figure 4 illustrates the relationship between the number of active users and the BER for both the SDD technique and the NAND subtraction technique. It can be easily seen that at a BER of  $10^{-9}$ , the SDD technique supports 365 users, while the NAND subtraction technique supports 150 users only. Therefore, the SDD technique provides a better performance and supports larger number of users than the NAND subtraction technique.

### 5.3 Relationship Between Received Power and BER

Figure 5 shows the relationship between the effective power received from each user and the BER, when the number of active users is equal to 40. It can be observed, that at BER of  $10^{-9}$ , the SDD technique needs ( $P_{sr} = -19$  dBm), while the NAND subtraction technique requires ( $P_{sr} = -17$  dBm), which is due to the PIIN still existing in the system. So, additional 2 dBm are required for NAND subtraction compared to SDD to support the same number of users.

### 5.4 Relationship Between PIIN Noise and Effective Power Received

Figure 6 illustrates the relationship between the PIIN and the effective power received from each user. When the code weight is increased, the received power is also increased,

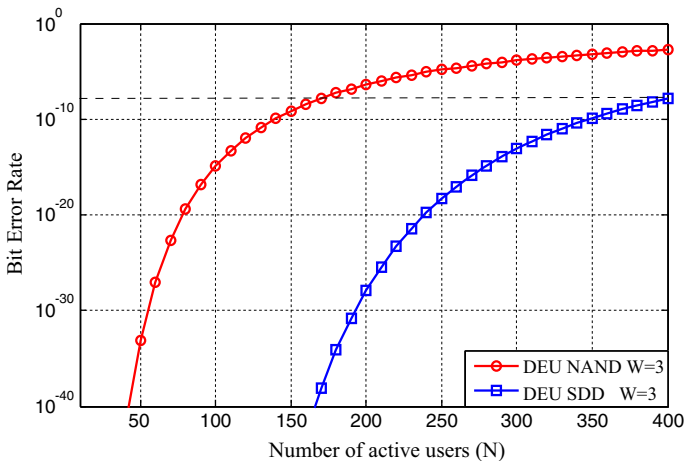


Fig. 4 BER versus the number of active users when  $P_{sr} = 10$  dBm  $N_B = 7$

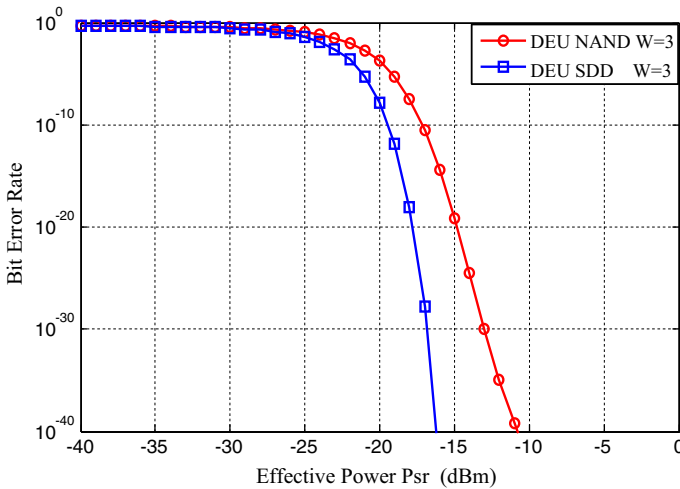


Fig. 5 BER versus the effective power received from each user when the number of users = 40

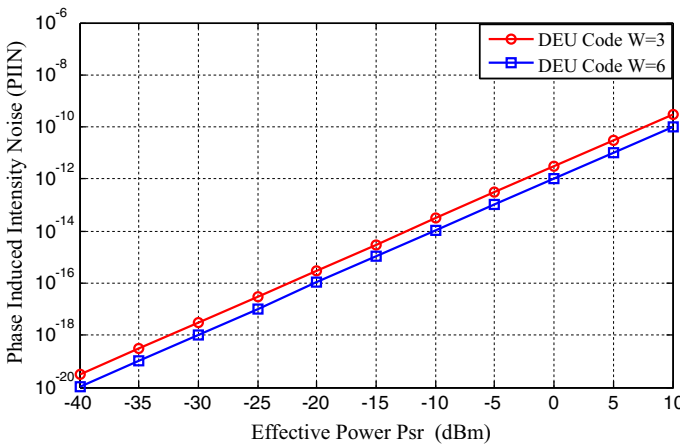


Fig. 6 PIIN versus effective received power from every user, where the number of users is 40

and the PIIN is increased, linearly. Because the PIIN is relevant to the MAI produced from overlapping of spectra from various users in the system, it is introduced from incoherent light fields that are mixed and incident upon a photo-detector.

### 5.5 Relationship Between SNR, BER, and Bit Rates

Figures 7 and 8 show bit rate versus SNR and BER, where the number of active users is equal to 60 and the effective power received is  $-10$  dBm. It can be seen that as the bitrate is increased, the system performance is degraded as the pulse width becomes smaller and pulses become susceptible to dispersion effect. Overall, the SDD technique still provides a better performance than the NAND subtraction technique.

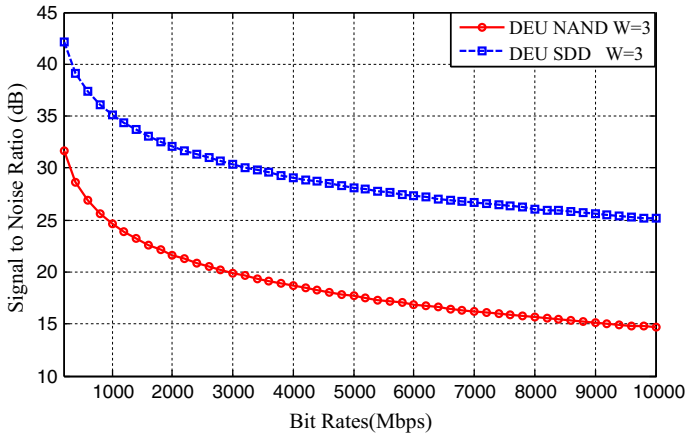


Fig. 7 SNR versus bit rate, when  $P_{sr} = -10$  dBm, and  $N = 60$

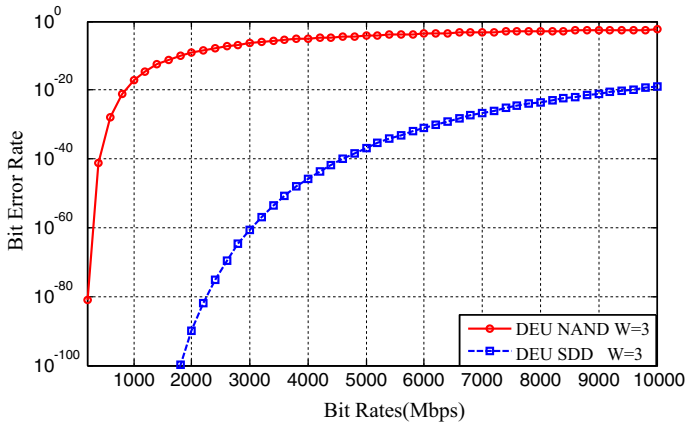


Fig. 8 BER versus bit rates, when  $P_{sr} = -10$  dBm and  $N = 60$

### 5.6 Relationship Between SNR, BER and the Number of Active Users with Variable Weight DEU Code

Figures 9 and 10 demonstrate the SNR and the BER versus the number of active users at various weights 2, 4, and 6. It can be observed that when the number of active users is increased, the system performance is deteriorated due to interference from other users. In Fig. 10, at BER of  $10^{-12}$  and  $W = 6$ , the number of active users equals 90. At BER of  $10^{-9}$  and  $W = 4$ , the number of active users is 60. At a BER of  $10^{-3}$  and  $W = 2$ , the number of active users is 50. Therefore, users can support different QoS values by changing the code weight, because the high weight means a better performance due to the high power received and the larger number of users that can be supported.

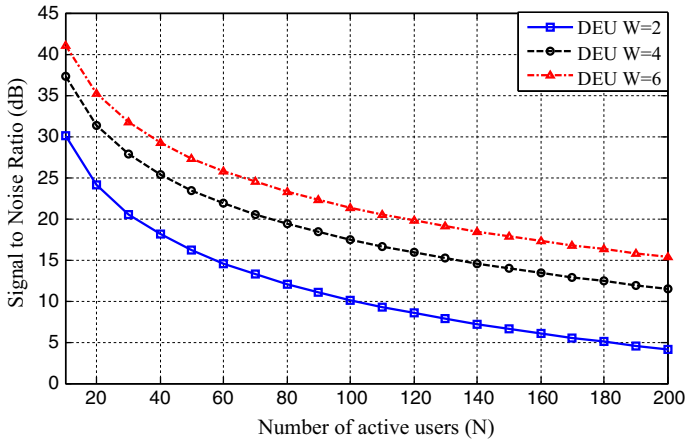


Fig. 9 SNR versus the number of active users for variable weight DEU code using the SDD technique

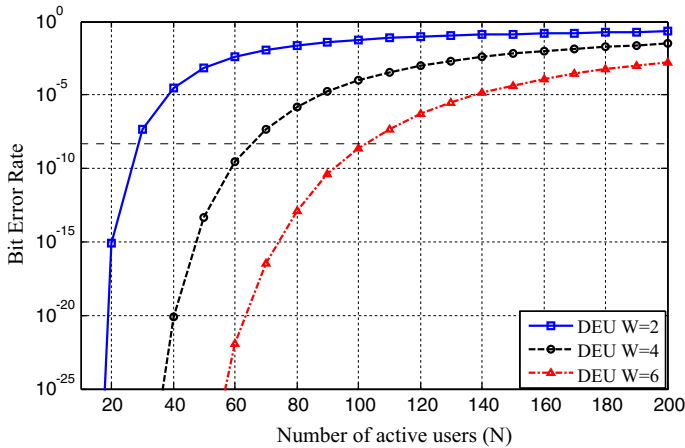
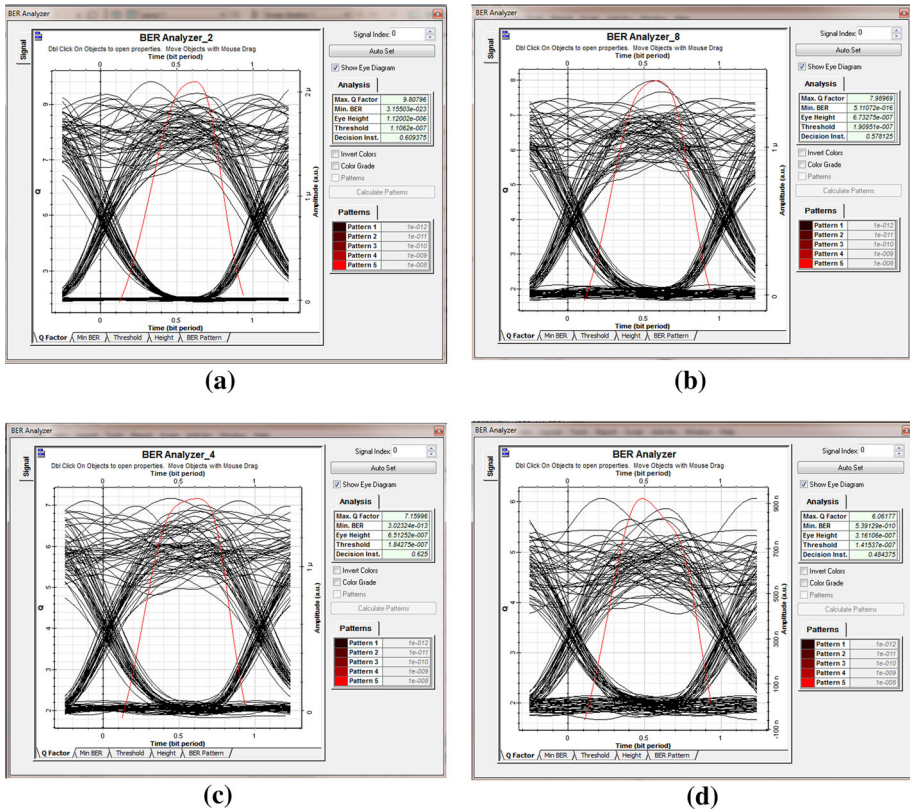


Fig. 10 BER versus the number of active users for variable weight DEU code using the SDD technique

### 6 Network Simulation

Optisystem version.13 has been used to simulate the performance of the DEU code with the SDD technique for 8 users. Tests have been carried out using a white light source with a spectral width of 0.8 nm, at a bit rate equal to 622 Mbps. ITU-T G.652 standard for Single-Mode optical Fiber (SMF) at 40 km has been adopted with attenuation of 0.25 dB/Km, polarization mode dispersion of 16.75 ps/nm km, and nonlinear effects according to the typical industry values. At the receiver side, the dark current is set to 5 nm, and the thermal noise co-efficient is set to  $1.8 \times 10^{-23}$  W/Hz for each photo-detector. Figure 11a shows that the eye diagram of the DEU code with the SDD technique, where the SDD technique gives a low BER of  $10^{-23}$ . Figure 11 also shows a simulation for 12 users with





**Fig. 11** Eye diagrams for DEU code. **a** Eye diagram of DEU code with SDD for 8 users,  $W = 4$ . **b** Eye diagram for VW-DEU code,  $W = 6$ . **c** Eye diagram for VW-DEU code,  $W = 4$ . **d** Eye diagram for VW-DEU code,  $W = 2$

variable weights of 2, 4, and 6 for different services as explained in Sect. 2.1. As shown in Fig. 11b, c, users with high weight have better BER and large open eye patterns.

## 7 Conclusion

The OCDMA system provides improved performance with SAC-OCDMA codes. The DEU code is one of the most promising codes to use in future optical networks. It has an ideal cross correlation, a simple construction, the ability to support a large number of users, and the free cardinality in selecting the code weight and the number of users. The SDD gives superior performance over all other detection techniques due to its eradication to both MAI and PIIN, and it needs low hardware complexity and cost but provides poor treatment to MAI. On the other hand, the NAND subtraction technique provides the best performance among all other subtraction techniques such as complementary, XOR and AND, but these techniques increase the receiver complexity and cost. However, it provides excellent treatment to the MAI problem by using the full weight of the code sequence. It is noticed that the users with higher weights achieve better performances than those with lower

weights in the variable weight system. So, supporting different QoS triple-play services is possible. In the future studies, supporting multiple rates and QoS values depending on code length weight should be investigated.

## References

1. Prucnal, P. (2006). Optical code division multiple access fundamentals and applications, 2006.
2. Ahmed, N., Aljunid, S. A., Fadil, A., Ahmed, R. B., & Rashid, M. A. (2013). Performance enhancement of OCDMA system using NAND detection with modified double weight (MDW) code for optical access network. *Optik - International Journal for Light and Electron Optics*, 124(13), 1402–1407.
3. Ahmed, H. Y., & Nisar, K. S. (2013). Diagonal Eigenvalue unity (DEU) code for spectral amplitude coding-optical (Vol. 19, no. 4, pp. 335–347). Amsterdam: Elsevier.
4. Abdullah, M. K., Hasoon, F. N., Aljunid, S. A., & Shaari, S. (2008). Performance of OCDMA systems with new spectral direct detection (SDD) technique using enhanced double weight (EDW) code. *Optics Communications*, 4658–4662.
5. Norazimah, M. Z., Aljunid, S. A., Fadhil, H. A., & Md zain, A.S. (2011). Analytical comparison of various SAC-OCDMA detection techniques. In *2011 IEEE 2nd international conference on photonics (ICP)*.
6. Seyedzadeh, S., Sahbudin, R. K. Z., Abas, A. F., & Anas, S. B. A. (2013). Weight optimization of variable weight ocdma for triple-play services. In *2013 IEEE 4th international conference on photonics (ICP)*, Melaka.
7. Djordjevic, I. B., Vasic, B., & Rorison, J. (2004). Multi-weight unipolar codes for multimedia spectral-amplitude-coding optical CDMA systems. *IEEE Communications Letters*, 8(4), 259–261.
8. Nasaruddin, N., & Tsujitoka, T. (2008). Design of strict variable-weight optical orthogonal codes for differentiated quality of service in optical CDMA networks. *Computer Networks*, 52(10), 2077–2086.
9. Junita, M. N., Aljunid, S. A., Anuar, M. S., Arief, A. R., Rahim, R.A., Ahmed, R. B., & Saad, M. N. (2012) Modeling and simulation of variable weight zero cross correlation code in optical access network. In *3rd international conference on photonics*, Penang.
10. Fadhil, H. A., Aljunid, S. A., & Badlisha, R. (2009). Triple-play services using random diagonal code for spectral amplitude coding OCDMA systems. *Journal of Optical Communications*, 30(3), 155–159.
11. Anas, S. B. A., Abdullah, M. K., Mokhtar, M., Aljunid, S. A., & Walker, S. D. (2009). Optical domain service differentiation using spectral-amplitude-coding. *Optical Fiber Technology*, 15(1), 26–32.
12. Kakaee, M. H., Seyedzadeh, S., Fadhil, H. A., Anas, S. B. A., & Mokhtar, M. (2014). Development of multi-service (MS) for SAC-OCDMA systems. *Optics & Laser Technology*, 49–55.
13. Wei, Z., Shalaby, H. M. H., & Ghafouri-Shiraz, H. (2001). Modified quadratic congruence codes for fiberBragg-grating-based spectral-amplitude-coding optical CDMA systems. *Journal of Lightwave Technology*, 19 (9), 1274–1281.



**Salwa Mostafa** was born in Menoufia, Egypt, in 1990. She received the B.Sc. degree in Electronics and Electrical Communications Engineering from Faculty of Electronic Engineering, Menoufia University, Egypt, in 2012. In 2012, she joined the Department of Electronics and Electrical Communications Engineering, Menoufia University as a Lecturer. Her current research interests include optical code division multiple access, free space optics and indoor wireless communication.



**Abd El-Naser A. Mohamed** received Ph.D. degree from the faculty of Electronic Engineering, Menoufia University in 1994. Now, his job career is Assoc. Prof. Dr. in Electronics and Electrical Communication Engineering department. Currently, his field and research interest in the optical communication Networks, and digital communication systems.



**Fathi E. Abd El-Samie** received the B.Sc. (Honors), M.Sc., and Ph.D. degrees from Menoufia University, Menouf, Egypt in 1998, 2001 and 2005 respectively. Since 2005, he has been a teaching staff member with the Department of Electronics and Electrical Communications, Faculty of Electronic Engineering, Menoufia University. He worked as a researcher at KACST-TIC in radio frequency and photonics for the e-Society (RFTONIC). He is a co-author of about 200 papers in international conference proceedings and journals and 4 textbooks. His current research interests include image enhancement, image restoration, image interpolation, superresolution reconstruction of images, data hiding, multimedia communications, medical image processing, optical signal processing, and digital communications. Dr. Abd El-samie was a recipient of the Most Cited Paper Award from the Digital Signal Processing journal in 2008.



**Ahmed Nabih Zaki Rashed** was born in Menouf city, Menoufia State, Egypt country in 23 July, 1976. Received the B.Sc., M.Sc., and Ph.D. scientific degrees in the Electronics and Electrical Communications Engineering Department from Faculty of Electronic Engineering, Menoufia University in 1999, 2005, and 2010 respectively. Currently, his job carrier is a scientific lecturer in Electronics and Electrical Communications Engineering Department, Faculty of Electronic Engineering, Menoufia university, Menouf. Postal Menouf city code: 32951, EGYPT. His scientific master science thesis has focused on polymer fibers in optical access communication systems. Moreover his scientific Ph. D. thesis has focused on recent applications in linear or nonlinear passive or active in optical networks. His interesting research mainly focuses on transmission capacity, a data rate product and long transmission distances of passive and active optical communication networks, wireless communication, radio over fiber communication systems, and optical network security and management. He has published many high scientific research papers in high quality and technical international journals in the field of advanced communication systems, optoelectronic devices, and passive optical access communication networks. His areas of interest and experience in optical communication systems, advanced optical communication networks, wireless optical access networks, analog communication systems, optical filters and Sensors. As well as he is editorial board member in high academic scientific International research Journals. Moreover he is a reviewer member in high impact scientific research international journals in the field of electronics, electrical communication systems, optoelectronics, information technology and advanced optical communication systems and networks.

lished many high scientific research papers in high quality and technical international journals in the field of advanced communication systems, optoelectronic devices, and passive optical access communication networks. His areas of interest and experience in optical communication systems, advanced optical communication networks, wireless optical access networks, analog communication systems, optical filters and Sensors. As well as he is editorial board member in high academic scientific International research Journals. Moreover he is a reviewer member in high impact scientific research international journals in the field of electronics, electrical communication systems, optoelectronics, information technology and advanced optical communication systems and networks.